ABSTRACT

Title of Document: THE NEURAL DYNAMICS OF AMPLITUDE MODULATION PROCESSING IN THE HUMAN AUDITORY SYSTEM

Kai Sum Li, MS, 2010

Directed By: Professor Jonathan Z. Simon, Department of Electrical and Computer Engineering

The neural, auditory amplitude modulation transfer function (MTF) is estimated from 3 – 50 Hz using magnetoencephalography (MEG). All acoustic stimuli are amplitude modulated (AM). Two different dynamical stimulus types are used: exponential sweeps with the AM rate changing from 2 up to 60 Hz, and 89 down to 3 Hz. Several carriers are also employed, including 3 pure-tone carriers (250 Hz, 707 Hz and 2 kHz) and 3 bandlimited pink-noise carriers (1/3, 2 and 5 octaves centered at 707 Hz). Neural response magnitudes, phases, group delays and impulse responses are all estimated. Our results show that the shape of modulation transfer function is flat but with a slightly low pass shape below 10 Hz. The phase of the response is approximately linear in many frequencies. The group delay is around 50 ms at 40 Hz for increasing-frequency sweeps and closer to 100 ms for decreasing-frequency sweeps.

THE NEURAL DYNAMICS OF AMPLITUDE MODULATION PROCESSING IN THE HUMAN AUDITORY SYSTEM

By

Kai Sum Li

Thesis submitted to the Faculty of the Graduate School of the
University of Maryland, College Park, in partial fulfillment
of the requirements for the degree of
Master of Science
2010

Advisory Committee:
Professor Jonathan Z. Simon, Chair
Professor Richard J. La
Professor Timothy Horiuchi

Dedication

To my family and friends

Acknowledgements

I would like to express my gratitude to the following individuals/groups:

1. Professor Jonathan Simon. The one who grants me this opportunity to work in his lab and teaches me everything in the research field. I am sure I will not be able to finish this thesis without his help.
2. Nai Ding, Marisel Villafane Delgado and Nicholas Asendorf. They collaborate with me to finish this study. While Nai suggests valuable suggestions to the analysis, Marisel and Nicholas record half of the data and use a different analysis method to compare our results. Their help is what make this thesis complete.
3. All the past and present members of Computational Sensorimotor Systems Lab, including Nai Ding, Marisel Villafane Delgado, Nicholas Asendorf, Dan Hertz and Jiachen Zhuo. All of them provide valuable opinions on this study.
4. My family, especially my parents and my sister. They are the one who support me without any doubts.

Table of Contents

List of Tables

List of Figures

Chapter 1: Introduction

1.1 Magnetoencephalography (MEG)

The human brain is one of the most complex structures in the human body. There are at least 10^{10} neurons in the cerebral cortex. They connect to each other to construct a vast network. When information is transmitted between two cells, small currents flow in the system and project a weak magnetic field. Single cell activity is normally too weak to be measured; however, if thousands of nearby neurons transmit at the same time, the amplified magnetic field is strong enough to be measured by a SQUID (Superconducting quantum interference device) magnetometer placed outside the skull. This method of recording brain signals is called Magnetoencephalography (MEG), which is one of the few methods that can measure brain activity noninvasively.

1.1.1 Simple neural mechanisms

A neuron consists of cell body (the soma), which contains the nucleus; the dendrites, which are extensions to receive information from other cells; and the axon, which is a long fiber that transmits impulses to other cells. The cells that we are interested are called pyramidal and stellate cells. The dendrites of these types may be perpendicular to the cortical surface. When these cells are stimulated, they send out electrical pulses to other neurons. In order to create a magnetic field that is strong enough to be measured by MEG, it is estimated that (Hamalainen et al 1993) a million synapses (connections) must be simultaneously active at the same time. Since there are approximately 10^5 pyramidal cells per mm^2 and thousands of synapses per cells, only a few synapses out of a thousand are needed to be activated in an area of 1 mm^2 to produce a measurable signals. In practice, a larger activation area is needed because the magnetic field may partially be cancelled out by other areas.

1.1.2 Advantages of MEG

One of the main advantages using MEG is its temporal resolution. The time resolution of MEG is better than 1 ms, which make it a perfect tool to measure temporal information of the brain using rapidly changing stimuli. The spatial resolution is, under favorable circumstances, 2-3 mm for sources in the brain. This is done by approximately modeling the magnetic fields using current dipoles. Since the magnetic field generated by the brain is weak (10^{-15} Tesla) (the magnetic field of the Earth is ~0.5×10^{-4} Tesla), several methods are normally used to avoid contamination of the signals. Typically, the recordings will be done in a magnetically shielded room. All magnetic materials must be removed inside the room. The sensors are also made to be only sensitive to the magnetic field close to them so that other biological artifacts will have less effect on the measurement.

MEG can be used for detecting evoked and ongoing brain activities. The evoked responses, elicited by abrupt sensory stimuli, can be extracted from the background by averaging the measured signals. The evoked activity contains distinct rhythmic components around 10, 20 and 40 Hz (Hari et al 2000). These kinds of activities are ideal for MEG because of their fast changing nature. Blood-flow-related imaging methods, such as PET and fMRI, will not be able to capture this kind of rapid changing activities. In our study, MEG is used to measured a more prolong response in our brain – auditory steady state response (aSSR).

1.2 The auditory steady state response (aSSR)

The auditory steady state response (aSSR), sometimes also referred as amplitude-modulation-following response (AMFR) (Aoyagi et al 1993a,b,c; Schoonhoven et al 2003) is an evoked potential (or evoked field) which sustains a constant frequency and phase (Regan 1989, Picton et al 2002). Using MEG, one can record aSSR by measuring the weak magnetic field generated by the brain (Hamalainen et al 1993). Numerous studies have investigated aSSR using different stimuli (Roβ et al 2000, Picton et al 2002). The most investigated area is the 40-Hz peak of the amplitude modulation transfer function (MTF). It is a prominent response at 40 Hz when the amplitude/power of the response is plotted against the corresponding modulation frequency. Because of its strong response, frequencies around 40 Hz have been used to measure other effects of the auditory system such as attention and scene analysis. Different theories have been proposed by different groups to explain the origin of aSSR and the prominent 40 Hz responses. Galambos et al 1981, the first group to discover the peak at 40 Hz, suggests that it represents the coalescence of the middle latency responses (MLB). Many other studies support this idea (Makeig 1990, Plourde et al 1991, Suzuki et al 1994). However, the origin of the peak is still arguable. Besides the 40-Hz region, other aspects of aSSR have also been investigated. Sleep has been shown to have a profound effect on the electrical activity of the brain. In the frequency range below 70 Hz, awake subjects have a stronger responses compared to sleeping subjects (Purcell et al 2004). On average, the strength of the responses in sleeping subject is reduced by half (Picton et al 2002). Above 70 Hz, steady state responses are less affected by sleep. Different types of carriers have also been investigated (Picton et al 2002, Purcell et al 2004). White noise carriers generally evoke a stronger response compared to pure-tone carriers (Picton et al 2002). However, some studies also have evidence that bandlimited noise give an even stronger response. Power et al (2007) suggested that bandlimited noise stimulates a more substantial area of auditory cortex than a modulated tone and at the same time stimulates more specific neural pathways than broadband noise. It is also suggested that the auditory cortex may be "periodotopically" organized instead of tonotopically organized. (Jones 2006). Thus, bandlimited signal may be an efficient stimulus.

1.3 Importance of the low frequency region in the MTF

Although aSSR has been investigated for a long time, the low frequency region of MTF (below 40 Hz) is still ambiguously described. Some studies (Rees et al 1986, Picton et al. 1987, Maiste et al 1989) attempt to estimate the MTF and group delay in the low frequency regions, but an accurate estimate is still missing. The main reason is that cortical responses in the low frequency band are severely contaminated by neural noise. Although it is difficult to measure, low modulation rate is an important building block for speech perception (Poeppel 2003). Envelope information, both frequency modulated and amplitude modulated, is a crucial features for capturing necessary information from speech (Xiang et al 2005). Different temporal codings have been investigated to understand the way the human brain encodes such modulations (Ding et al 2009, Luo et al 2007). Thus, it is of particular interest to investigate low frequency MTF in order to have a better understand of speech perception. A more recent EEG study (Alaerts et al 2009) uses stationary speech-weighted noise as the carrier and shows a prominent 20-Hz peak in the range of 4 – 32 Hz. However, MEG studies in this frequency range are still missing.

1.4 Our study of MTF below 40 Hz

In our study, MEG is used to record the low frequency “instantaneous” aSSR. The term “instantaneous” aSSR is used here because the stimuli in our study are not traditional constant AM-rate signal, but AM-rate sweeping through different frequencies. This kind of sweeping method has been used successfully in different studies, including visual and auditory (Picton et al 2002, Artieda et al 2003). It allows us to measure the aSSR over a large number of different parameter (in this study, the parameter is frequencies) in a short period of time. Instead of making multiple separate recordings at different parameters, the subjects can listen to one recording when the parameters of the stimulus change continuously. In such studies, all of the sweeps are linear sweeps. Our experiment uses exponential sweeps instead of linear sweeps to emphasize the low frequency band. Two experiments are carried out. The first experiment focuses on pure-tone carriers and the second experiment focuses on pink-noise carriers. Pink noise with different bandwidths are used in the experiment to explore the effect using different carriers. (Picton et al 2002).

Chapter 2: Methods

2.1 Subjects

12 subjects (5 Female) participated in the first experiment using pure-tone carriers. 1 additional subject participated but was not included because of too many recordings artifacts. Throughout this paper they are referred to as group 1. 13 subjects (2 Female) served in the second experiment using pink-noise carriers. They are identified as Group 2. 2 subjects (1 female) participated in both experiments. All participants were right handed and reported normal hearing and no history of audiological or neurological abnormalities. The experimental procedures were approved by the University of Maryland institutional review board. After the nature of the experiment was fully explained, written informed consent was obtained from each subject before the experiment started.

2.2 Stimuli

9 stimulus conditions are considered in both groups. All of them were generated using MATLAB (MathWorks Inc, Natick, MA). Stimuli in Group 1 all use pure-tone carriers and those in Group 2 use pink-noise carrier. The same exponential sweeps of the AM rate are used in both groups. The instantaneous frequency of the AM sweeps are given by:

$$rate_{up}(t) = 2 + 3^{0.37t} \qquad (0 \le t \le 11\text{s}) \tag{1}$$

$$rate_{down}(t) = 2 + 3^{0.37(10-t)} \qquad (0 \le t \le 11\text{s}) \tag{2}$$

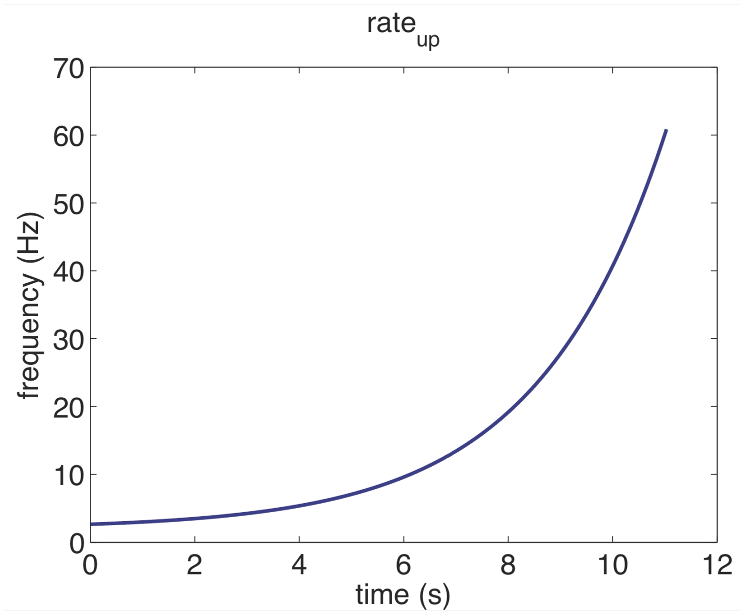

Figure 1: $rate_{up}(t)$. Modulation rate plotted against time t for up sweep stimuli. The rate increases from 2.66 Hz up to 60.14 Hz.

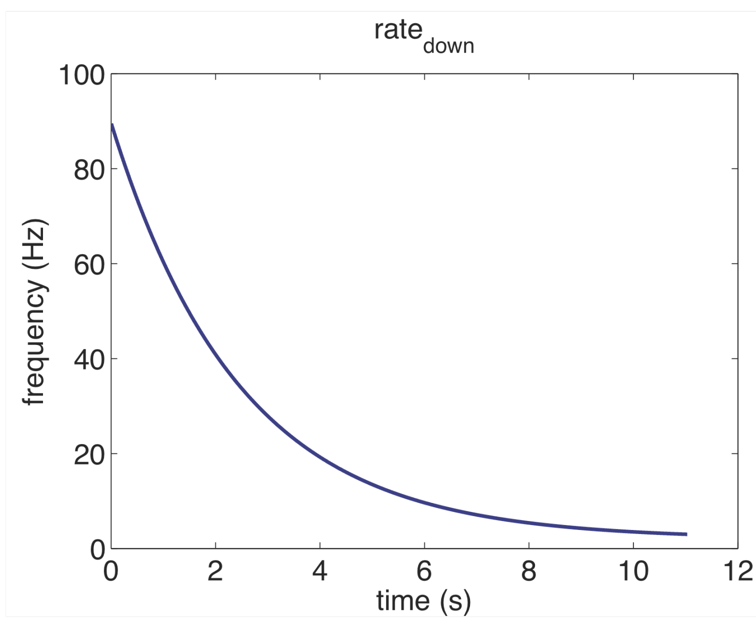

Figure 2: $rate_{down}(t)$. Modulation rate plotted against time t for down sweep stimuli. The rate decreases from 89.29 Hz down to 3 Hz exponentially.

Therefore rates range from 2.66 up to 60.14 Hz for up sweep stimuli (Figure 1) and from 89.29 down to 3 Hz for the down sweep stimuli (Figure 2). By taking the integral of the above function with respect to time and adding 1 to the function (Artieda et al 2003), the envelopes of the signal are calculated (Farina 2000). The envelopes are also multiplied by ½ so that they vary from 0 to 1. Mathematically, the envelopes were given by:

$$chirp_{up}(t) = \frac{1}{2}(1 + \sin(2\pi(2t + \frac{1}{0.37(\ln 3)}3^{0.37t}))) \tag{3}$$

$$chirp_{down}(t) = \frac{1}{2}(1 + \sin(2\pi(2t - \frac{3^{3.7}}{0.37(\ln 3)}3^{-0.37t}))) \tag{4}$$

Each of the above chirps corresponds to 3 stimuli for each experiment. These envelopes were multiplied by each carrier to generate each acoustic stimulus. In experiment 1, the carriers were pure-tone carriers with frequencies 250 Hz, 707 Hz and 2 kHz. In experiment 2, the carriers were pink noise with bandwidth of 1/3, 2 and 5 octaves centered at 707 Hz. Each stimulus was repeated 20 times. The remaining three stimuli had a constant AM rate of 3 Hz, 13 Hz, and 37 Hz with a pure-tone carrier frequency of 707 Hz. They were repeated 10 times. They are referred as constant-rate stimuli. The modulation depth of all the stimuli above is 95%. So, in this investigation, a total of 18 different stimuli are used (Table 1). Before the main experiment, all subjects participated in a preliminary test, listening to 1 kHz pure tones repeated 100 times (each duration 50 ms). These responses are used to verify that the subject is positioned properly in the machine that signals from auditory cortex has a satisfactory signal to noise ratio (SNR).

	Modulation Style	Group 1 (Pure-tone carrier)	Group 2 (Pink-noise carrier)
Stimulus 1	Up sweep	250 Hz carrier	1/3 octave carrier
Stimulus 2		707 Hz carrier	2 octave carrier
Stimulus 3		2 kHz carrier	5 octave carrier
Stimulus 4	Down sweep	250 Hz carrier	1/3 octave carrier
Stimulus 5		707 Hz carrier	2 octave carrier
Stimulus 6		2 kHz carrier	5 octave carrier
Stimulus 7	Constant AM rate	3Hz AM rate 707Hz carrier	3Hz AM rate 1/3 octave carrier
Stimulus 8		13 Hz AM rate 707 Hz carrier	13 Hz AM rate 2 octave carrier
Stimulus 9		37 Hz AM rate 707 Hz carrier	37 Hz AM rate 5 octave carrier

Table 1: Stimuli used in the experiments. 9 stimuli were used for each group (Column 2 and 3). They are divided by three groups of stimuli depending on their modulation type: up sweep, down sweep and constant AM rate (Column 1). Group 1 (Column 2) consists of stimuli with pure-tone carrier. Croup 2 (Column 3) consists of stimuli with a pink-noise carrier. Their frequencies/frequency ranges are listed in both columns.

2.3 MEG recording and analysis

The experiments are conducted using a 157-channel whole-head MEG system (5-cm baseline axial gradiometer SQUID-based sensors; KIT, Kanazawa, Japan).

Besides the 157 channels positioned around the head, three reference channels, positioned away from the subjects, are also used to measure environmental magnetic field. All recordings are conducted in a magnetically shielded room, sampled at 1 kHz. A 200-Hz low-pass filter and a notch filter at 60 Hz are applied online to remove the high frequency components and artifacts generated by the power grid. All subjects are instructed to close their eyes to reduce their eye movement throughout the recording process to reduce artifacts. Data analysis is applied offline after each experiment. All data goes through the same process. First, contaminated channels (recorded value was larger than 5000 pT or constant for more than 10% of the recorded time) and trials (0.5s out of 11s, i.e. 4.55% of the recorded values, were constant or >5000 pT) are first determined and not considered further in the studies. Then, the remaining data is denoised using TS-PCA (de Cheveigné and Simon 2007). This is a method to remove environmental noise by projecting the data to the external noise measuring reference channels. The projection is considered as part of the noise and thus is removed. After TS-PCA, data is passed through spatial filters synthesized by a blind source separation method known as denoising source separation (DSS), which removes other magnetic signals of uninteresting biological origin (de Cheveigné and Simon 2008a). The DSS components are then sorted based on what fraction of the response power is phase-locked to the stimulus. Only first component was kept for the later part of the analysis.

2.4 Extraction of Amplitude and Phase response

2.4.1 Constant AM rate response

Wavelet transform and Fourier analysis were both used in analyzing stationary responses generated by the constant rate stimuli. Since both methods generated similar results, the details of Fourier analysis will be omitted in this article. The wavelet transform is computed for the cortical response and averaged over all trials for each subject. Using the complex Morlet as the basis function, a scalogram is created for each experimental condition. A complex Morlet is defined as

$$\psi(x) = \frac{1}{\sqrt{\pi f_b}} e^{2i\pi f_c x} e^{-\frac{x^2}{f_b}} \tag{5}$$

where f_b is the bandwidth of the wavelet and f_c is the center frequency of the wavelet. In this study, we take $f_b = 20$ and $f_c = 1$ to give a good temporal and frequency resolution for our frequency range. After the wavelet transform is performed, a scalogram is created. For better interpretation, the scale of the scalogram, s, is converted to its corresponding frequency using the following equation

$$f = \frac{f_c}{sT} \tag{6}$$

where T is the sampling period. After this conversion, the wavelet transform will become a function of time τ and frequency f instead of time τ and scale s.

The results of the transformed response are then compared with the noise of that particular frequency, $\overline{P_{noise}(\tau, f)}$. This noise is taken as the cortical response of that frequency under different stimuli. For example, if 3 Hz is the target frequency, the noise at 3 Hz will be extracted from the 3 Hz trial. And the 3 Hz responses for 17 Hz and 37 Hz trials will be considered as the noise at 3 Hz. This is performed based on the assumption that the cortical responses $y(t)$ only exhibit neural response at the stimulus frequency, and only noise at other frequencies in different stimuli. The cumulative distribution function of the noise sample is then calculated and if the response at a certain frequency was over the 95 % of the noise distribution, the response is considered significant. This can get around the problem that noise in low frequency (<20 Hz) generally does not fit a Gaussian model in our experimental environment. After the significant test, the amplitude modulation transfer function (MTF) was given by

$$MTF(f) = 10\log_{10}\frac{\overline{Y_{WT}^{2}(\tau,f)} - \overline{P_{noise}(\tau,f)}}{P_{stimulus}(\tau,f)} \quad (7)$$

where $Y_{WT}(\tau,f)$ is the wavelet transform of a significant response $y(t)$ converted into frequency domain, $\overline{P_{\text{stimulus}}(\tau,f)}$ is the power of the stimulus and $\overline{P_{noise}(\tau,f)}$ is the averaged power of the noise for a particular AM frequency f. Here, f is equal to 3, 13 or 37 Hz.

The analysis of phases using wavelet transform is calculated as follow. Phase difference between the cortical response and the stimuli was first taken, i.e.

$$\theta(t,f) = \theta_{Y}(t,f) - \theta_{stimulus}(t,f) \quad (8)$$

where $\theta_{Y}(\tau,s)$ is the phase calculated from wavelet transform.

Then the circular mean phase at each target frequency, $\overline{\theta(f)}$ over trials i, is given by (Fisher, 2000)

$$\overline{\theta(f)} = \begin{cases} \tan^{-1}(S/C) & S>0,\ C>0 \\ \tan^{-1}(S/C)+\pi & C<0 \\ \tan^{-1}(S/C)+2\pi & S<0,\ C>0 \end{cases} \tag{9}$$

where $C = \sum_{i=1}^{n} \cos\theta_i$ and $S = \sum_{i=1}^{n} \sin\theta_i$

The sample circular standard deviation v is defined by (Fisher, 2000)

$$v = \sqrt{-2\log_e \overline{R}} \tag{10}$$

where $\overline{R} = \sqrt{C^2 + S^2}$

2.4.2 Exponential AM rate response

The method of using the wavelet transform in the exponential AM sweep is similar to the way of analyzing constant AM stimuli. However, since AM frequency varies now over time, a mask is used to extract the necessary information from the scalogram under different time periods. Since the aSSR generated by a SAM stimulus follows the AM frequency of the stimulus, the time period can be extracted using the AM frequency of the stimuli itself to detect target frequency. Specifically, the envelope of the stimulus is first extracted. Then a wavelet transform is generated from the envelope of the stimuli. A threshold is then set. All values below the threshold are set to 0 and all values above the threshold is set to 1. Using this method, a matrix with only 1s and 0s is created. So, for each frequency, a square window is generated over time. All the windows for each frequency cover different duration, which will be used to extract the target response at different time. Since our AM rate changed with exponential time, the window will be longer in the low frequency regions (~400ms) and become shorter when the AM rate increase

(~100ms). The mask is then applied to the scalogram of the response. Since the frequency of the AM signal followed an exponential function, the response will also give an exponential form. By adjusting the threshold, most of the relevant signal will be captured by the mask.

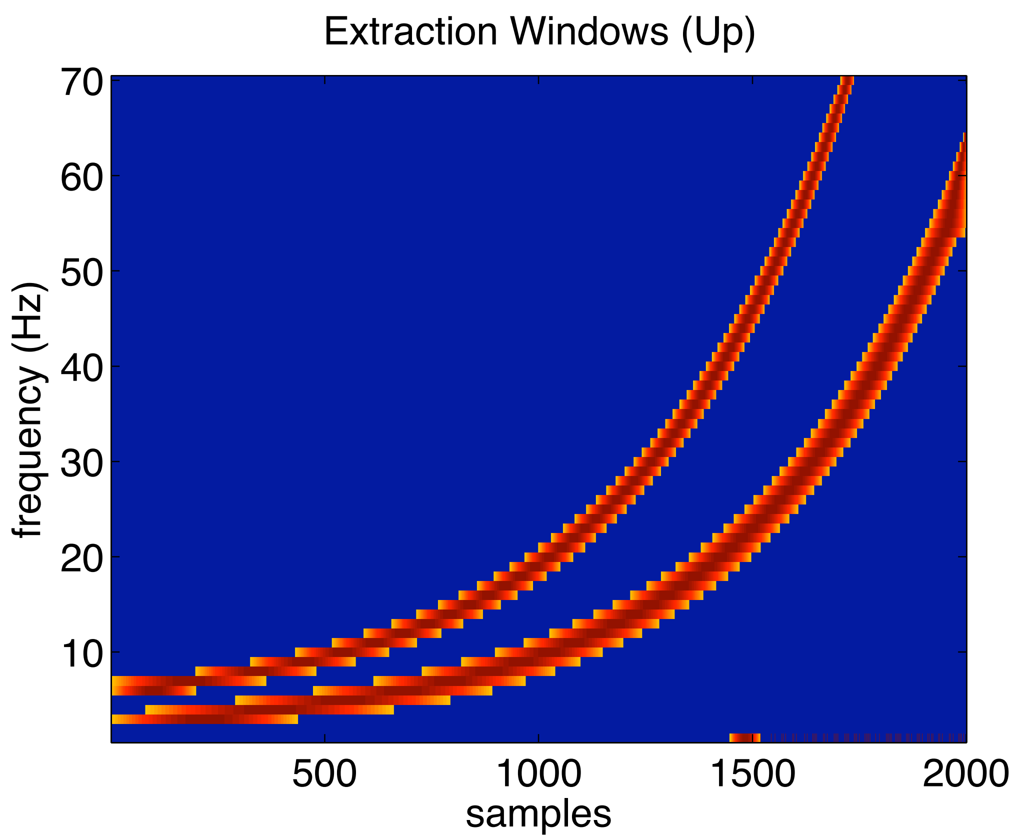

Figure 3: Extraction windows for up sweep stimuli. The lower red windows are used to capture the amplitude of the responses from the subjects at different time and frequencies. The blue regions of the graph are used to estimate the noise level. The upper red windows are used to capture the first harmonic of the response. Note that the harmonic responses not used in this study.

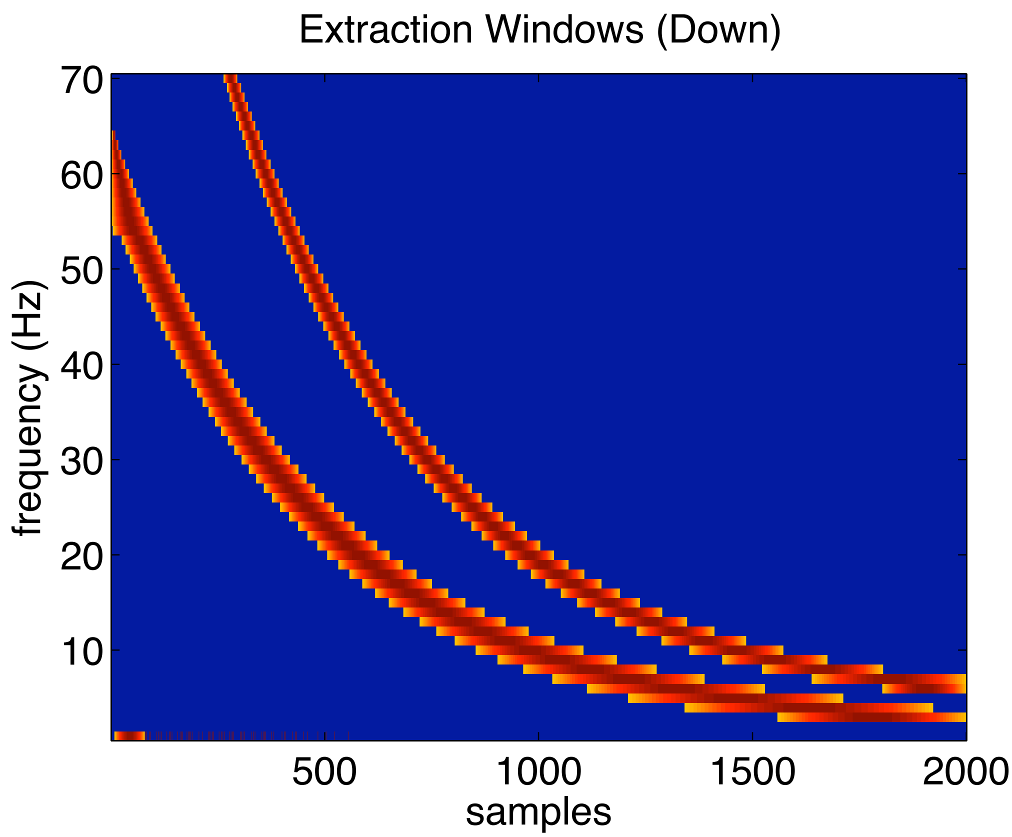

Figure 4: Extraction windows for down sweep stimuli. The lower red windows are used to capture the amplitude of the responses from the subjects at different time and frequencies. The blue regions of the graph are used to estimate the noise level. The upper red windows are used to capture the first harmonic of the response. Note that the harmonic responses not used in this study.

For each of the subjects, a significance test similar to the constant stimulus case is performed compared to the background noise $\overline{P_{noise}(\tau, f)}$. The noise sample is taken from a window when there is no ASSR, i.e. the 0s part of the mask. The first harmonics of the response are also excluded from the noise (Figures 3 & 4). There are more than 1300 samples taken in the low frequency region and around 1700 samples taken in the high regions. Since the distribution of the noise power in the low frequency region cannot be modeled by simple mathematical expression, the power of the noise was plotted for each frequency and the 95% was set as the threshold of the significant test. If the response of each subject at each frequency is lower than this threshold, it will not be further considered in the analysis. The amplitude response and phase response are then calculated. For amplitude response, the square window is modified by a Hamming window $W_{\text{hamming}}(f)$. The mean of the signal inside the window is calculated for each frequency by $\overline{W(f)Y_{WT}^2(\tau,f)}$. $\overline{P_{noise}(\tau,f)}$, the power of the noise, and $\overline{P_{stimulus}(\tau,f)}$, the power of the stimulus, are calculated in the same way by considering the same frequency at different time. MTF is then calculated in decibels. So

$$MTF(f) = 10\log_{10}\frac{\overline{W_{\text{hamming}}(f)Y_{WT}^2(\tau,f)} - \overline{P_{noise}(\tau,f)}}{\overline{W_{\text{hamming}}(f)X_{WT}^2(\tau,f)}} \tag{11}$$

where $X_{WT}(\tau,f)$ is the wavelet transform of the envelope of the stimulus converted to the frequency domain for every frequency *f*. Here, the power of the frequency is assumed to be biased by the noise and thus their difference is calculated to estimate the real response.

Phase is calculated using a square window so each phase is weighted the same. The phase of the scalogram of the stimulus and response at each sampling point of was extracted. Since the AM frequency of our stimuli is varying, the phase of the stimuli will also vary over time. To tackle this issue, the phase difference of the response and the stimuli are first calculated for each frequency. By calculating the phase difference between the response and the stimuli, the varying phase in the stimulus can be estimated. Then the circular mean of the each window is found. To further reduce the error, the adjacent frequency (±1 Hz) is also taken into consideration. In another words, a 3-point Hamming window in the frequency domain is created. Since discontinuous points in some of the graph are quite common, if the adjacent frequency points are missing, the weights of the Hamming window are adjusted to compensate the lost pieces of information. Thus, in the result, a graph with fewer discontinuous points can be found compared to the MTF. After this process, the weighted circular mean of the phase was taken as the phase at that frequency. It is then used to calculate the group delay of the system for that particular frequency by

$$\tau(f_0) = \frac{1}{2\pi} \frac{\partial \varphi(f)}{\partial f}\bigg|_{f_0} \tag{12}$$

Note the group delay is different from the traditional mathematical definition of group delay using short time Fourier Transform (STFT). A negative sign is not needed because of the Morlet wavelet, which uses a positive exponential (in contrast to the Fourier Transform, which uses a negative exponential).

The impulse response was also calculated using the amplitude and phase response calculated above. By using amplitude and phase response from 1-50 Hz, impulse response was generated using inverse Discrete Fourier Transform (IDFT). Note that amplitude and phase information at 1 and 2 Hz are missing in our study. Thus, they are set to 0 to complete the spectrum. Bootstrap BC_a (Efron B. et al 1998) is used to estimate the 95% confidence interval of the impulse response.

Chapter 3: Results

3.1 MTF of Group 1 (Pure-tone carrier)

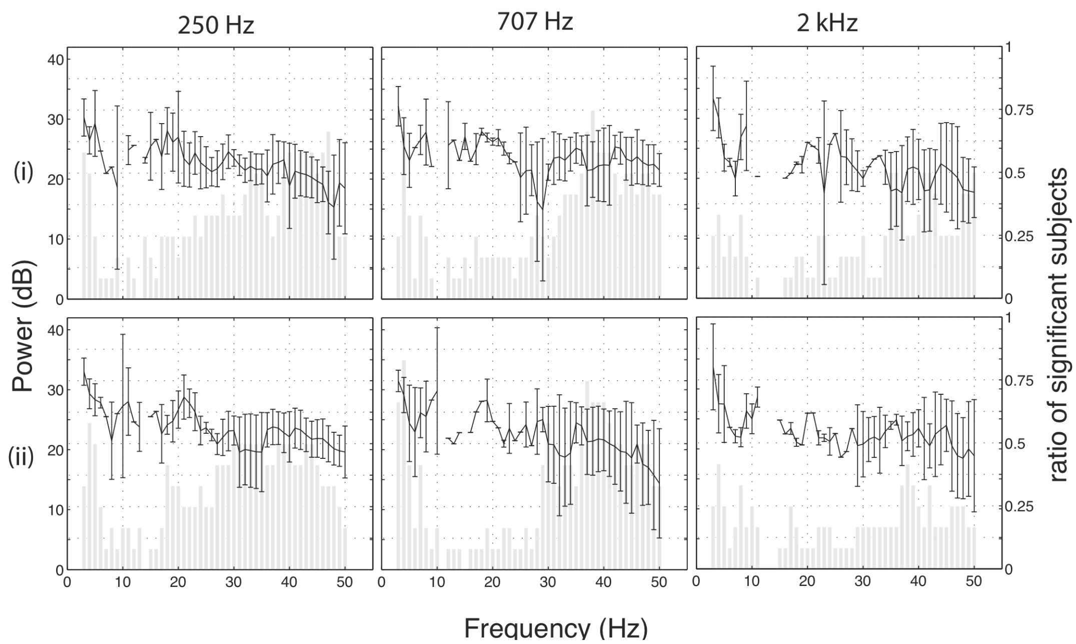

Figure 5: The modulation transfer functions (MTF) (averaged over subjects) for each dynamic stimulus with pure-tone carriers (and the relative subject contribution to each). The top row (i) is the MTF result from the up sweep stimuli and the bottom row (ii) is the result from down sweep stimuli. In light gray are the fraction of subjects whose responses were statistically significant (contributing to the MTF). Note that there are gaps in the modulation transfer functions when the number of contributing subjects drops to zero. The error bars represent the 95% confidence intervals. The maximum number of significant subjects for each frequency bin is 12.

Figure 5 shows the MTF averaged over all subjects for each pure-tone carrier. Each column corresponds to the 250 Hz, 707 Hz and 2 kHz pure-tone carrier. The upper row is the result of up sweep stimuli and the lower row is the result of down sweep stimuli. Only 3-50 Hz is shown because of the small window size of the analysis method and the effects of a hardware notch filter at 60 Hz. The bar chart on the same graph shows the fraction of subjects whose responses were statistically significant (contributing to the MTF) for each frequency. In group 1, the maximum number of subjects for each frequency is 12. Some frequency bins have no significant subjects and thus small gaps are found. If only 1 significant subject is found, there is no error bar. For extremely low frequency bins, like 4 or 5 Hz, the numbers of significant subject are large. However, beginning from 6 Hz, the number of significant subjects is reduced until 30 Hz. This result appears in all 6 conditions in group 1. Different carriers have no significant effects on the shape of MTF.

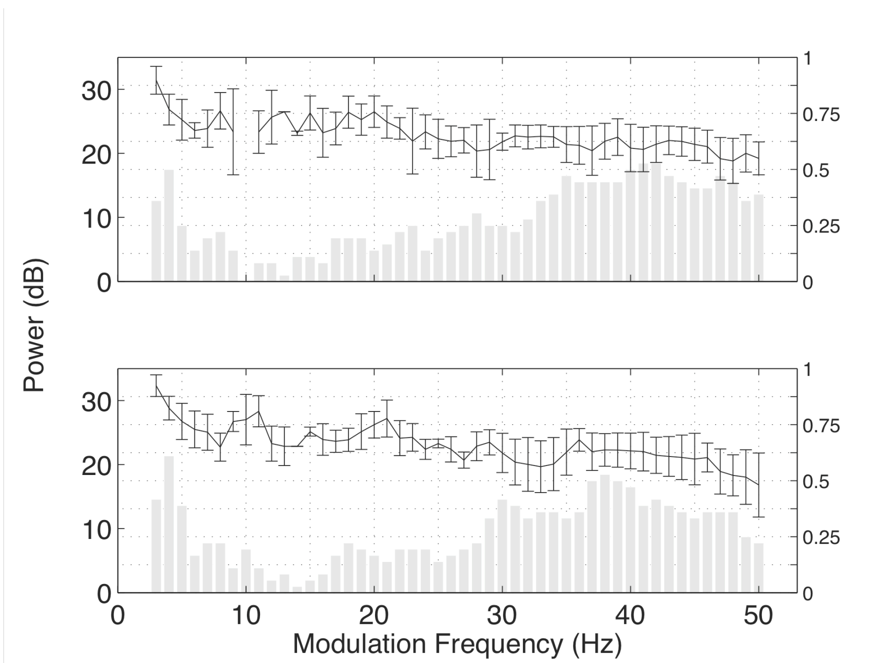

Figure 6: The modulation transfer functions (MTF) (averaged over different carriers) for each dynamic stimulus with pure-tone carriers (and the relative subject contribution to each). The top panel is the MTF result averaged over all up sweep stimuli and the bottom panel is the result from down sweep stimuli. In light gray are the fraction of subjects whose

responses were statistically significant (contributing to the MTF). The error bars are 95% confidence intervals. The maximum number of significant responses is 36 (12x3). The graph clearly show that around 50% of the subjects show significant responses in the frequency range of 30 - 50 Hz.

Since there is no significant difference between different pure-tone carriers, different sweeps are averaged together to increase the number of significant response for each frequency. Figure 6 shows the MTF for all subjects averaged over up sweep stimuli (upper panel) and down sweep stimuli (lower panel). The error bar in both graphs represents the 95 % confidence interval of the MTF. The bar chart on the same graph also shows the ratio of significant subjects for each frequency. In both graphs, the maximum number of significant subjects is raised to 36 (12x3). As we can see, the MTFs show a slightly low pass shape with strong response at 3-6 Hz and possibly 10 Hz. For the frequency in 6 - 20 Hz, the number of significant responses is low, which results in larger error bars.

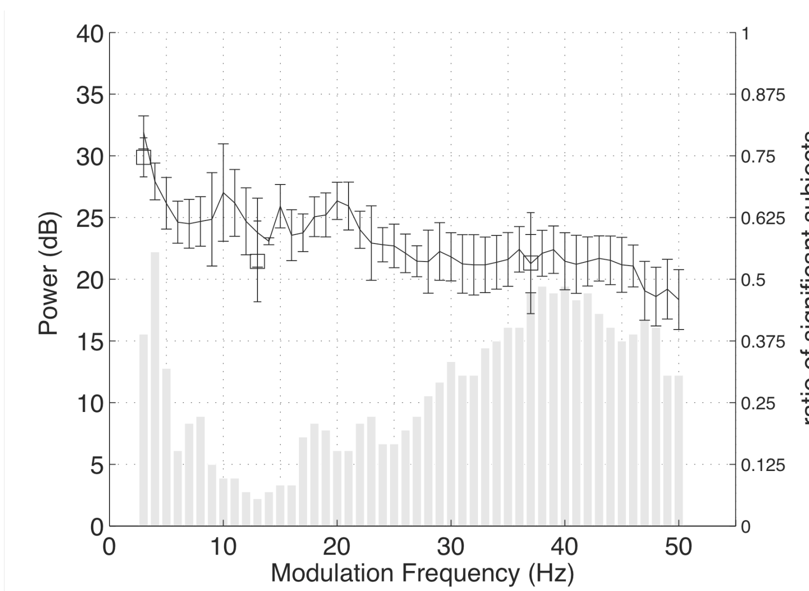

Figure 7: The modulation transfer functions (MTF) (averaged over sweeps) of pure-tone carriers (and the relative subject contribution to each). The error bars explain 95% of the confidence intervals. In light gray are the fraction of subjects whose responses were statistically significant (contributing to the MTF). The maximum number of significant responses is 72 (12x3x2). The results of constant rate-AM stimuli are also plotted at 3, 13 and 37 Hz using squares. Note that the results from sweep stimuli show no significant difference from the results of constant rate stimuli.

The data is further merged into one data set (Figure 7), which gives a total of 72 (12x3x2) subjects for every frequency. Constant AM rate results are also plotted on the same graph in Figure 7. They are marked as square at 3, 13 and 37 Hz. It can be seen that constant AM rate stimuli show no significant difference compared to the result from using the sweep at those frequencies. The graph still exhibits a slightly low pass from 3-6 Hz. Strong responses are also found around 10 Hz and 20 Hz, which result in two peaks around those frequencies.

3.2 <u>MTF of Group 2 (Pink-noise carrier)</u>

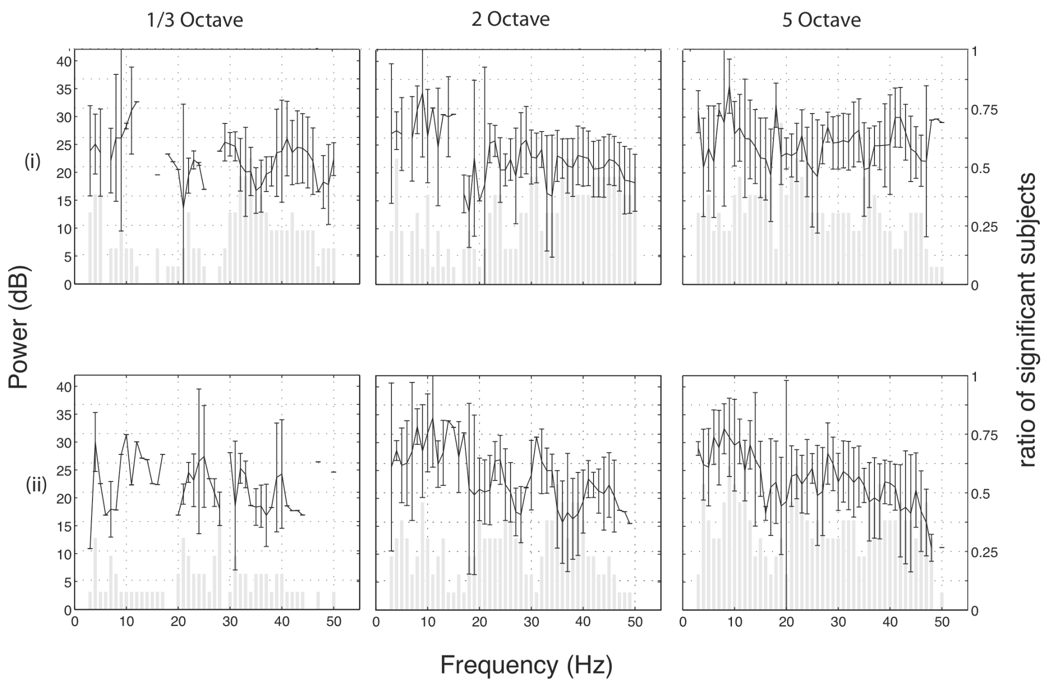

Figure 8: The modulation transfer functions (MTF) (averaged over subjects) for each dynamic stimulus with pink-noise carriers (and the relative subject contribution to each). The top row (i) is the MTF result from the up sweep stimuli and the bottom row (ii) is the result from down sweep stimuli. In light gray are the fraction of subjects whose responses were statistically significant (contributing to the MTF). Note that there are gaps in the modulation transfer functions when the number of contributing subjects drops to zero. The error bars represent the 95% confidence intervals. The maximum number of significant subjects for each frequency bin is 13.

Figure 8 shows the MTFs from subjects that have significant responses (Max: 13). Each response is averaged over subjects. The columns corresponds to 1/3, 2 and 5 octaves respectively. The upper panel of each column describes the MTFs using up sweep stimulus and the lower panel described the result of down sweep stimulus. At some frequencies, none of the subjects show a significant response compared to noise. Thus, it results in discontinuous points in the graph. In the cases of 1/3 octave (both up and down sweep), significant responses in the frequency range of 5 – 30 Hz are rare. Most of the frequency bins have less than 20% significant subjects. However, the situation improves with increasing octaves. This improvement appears in almost all frequencies. In general, there is no significant advantage of using down sweep stimuli compared to up sweep stimuli. Both up and down sweep have approximately same of significant subjects. For the MTFs, all conditions show a strong responses around 10 Hz. The shapes of the MTFs are slightly low pass at around 20 Hz.

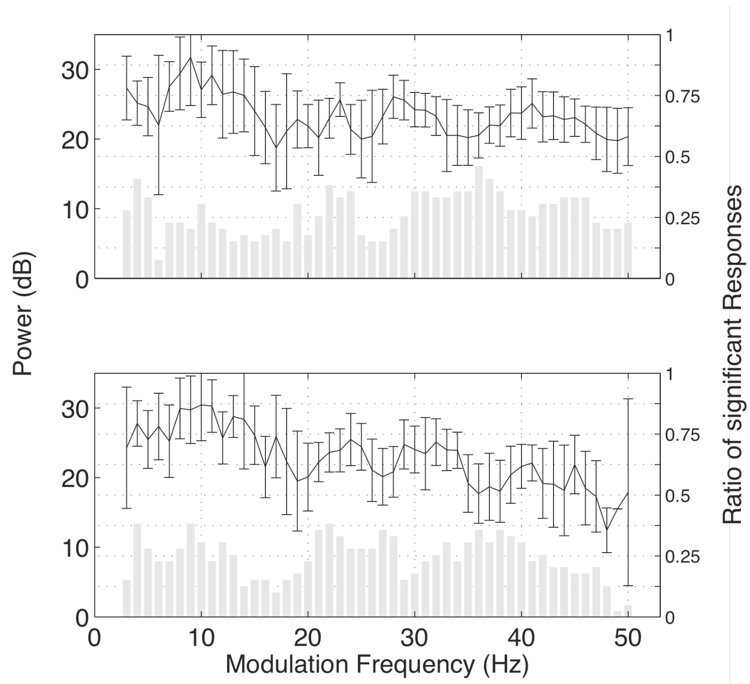

Figure 9: The modulation transfer functions (MTF) (averaged over carriers) for each dynamic stimulus with pink-noise carriers (and the relative subject contribution to each). The top panel is the MTF result from the up sweep stimuli and the bottom panel is the result from down sweep stimuli. In light gray are the fraction of subjects whose responses were statistically significant (contributing to the MTF). The error bars represent the 95% confidence intervals. The maximum number of significant subjects for each frequency bin is 39 (13x3). A strong response is found at around 8 – 12 Hz.

Figure 9 shows the MTF of 13 subjects averaged across different carriers. Upper panel is the average of all up sweep conditions and the lower panel is the average of all down sweep conditions. The total number of subjects is 39 (13x3). The error bars represent the 95% confidence intervals. A general strong response is observed in the low frequency region around 3 - 12 Hz.

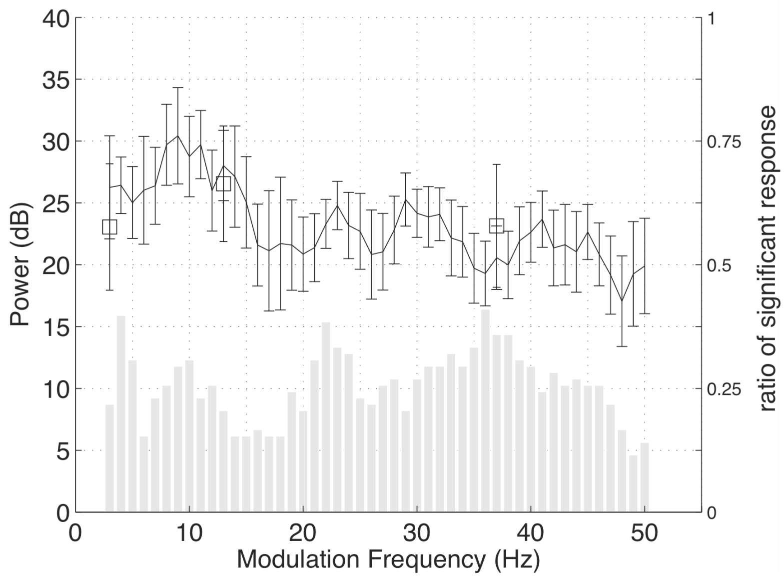

Figure 10: The modulation transfer functions (MTF) (averaged over sweeps). The relative subject contribution to each frequency is also plotted. The results of constant AM-rate stimuli were also plotted at 3, 13 and 37 Hz as squares. The error bars represent the 95% confidence intervals. In light gray are the fraction of subjects whose responses were statistically significant (contributing to the MTF). Similar to pure-tone carrier, there are no significant differences between the response of sweeps and constant-rate stimuli at those frequencies. The maximum number of significant subjects for each frequency bin is 78 (13x3x2). A strong response is found at around 3 – 12 Hz.

Similar to Group 1, the data is further merged and the result is plotted in Figure 10. The result of constant rate stimuli is also plotted on the same graph to compare the result. No significant difference is found in the frequencies selected here (3, 17 and 37 Hz). For each frequency bin, the maximum number of subjects is 78. The shape of the MTF is also slightly low pass, with a strong response from 3 – 12 Hz. Strong response can also be found around 25, 30 and 40 Hz.

3.3 Phases and group delay of Group 1 and Group 2

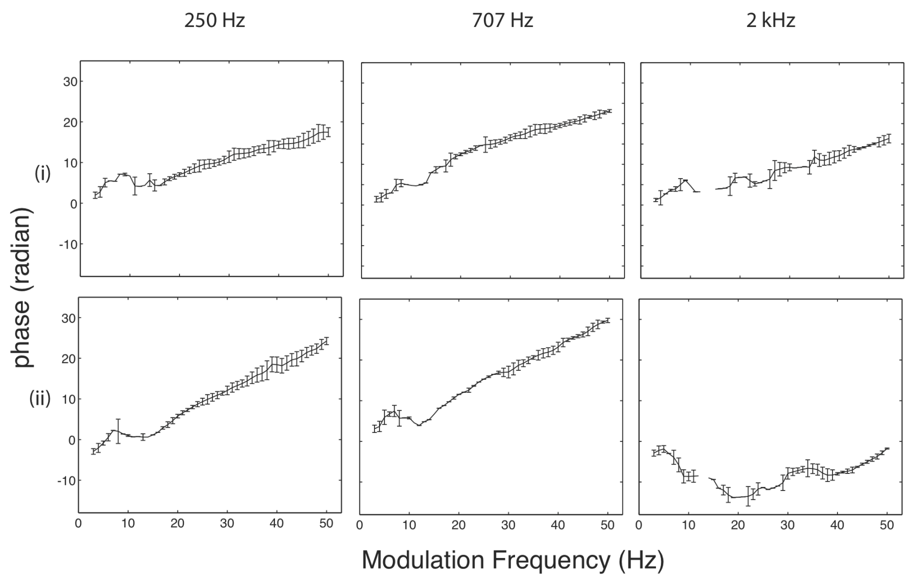

Figure 11: The phases (averaged over subjects) for each dynamic stimulus with pure-tone carriers. The top row (i) is the phase from the up sweep stimuli and the bottom row (ii) is the result from down sweep stimuli. Note that fewer gaps are found in all the results compared to Figure 5 because discontinuous points are estimated using their adjacent data (±1 Hz). The error bars represent the 95% confidence intervals.

The phase of the response for each condition in group 1 was plotted in Figure 11. The results were averaged over all subjects. All the graphs show that the phases are approximately linear for many frequencies. Since the carriers themselves have no significant impact on the phase. The results are grouped over up sweeps and down sweeps and the results are plotted in Figure 12.

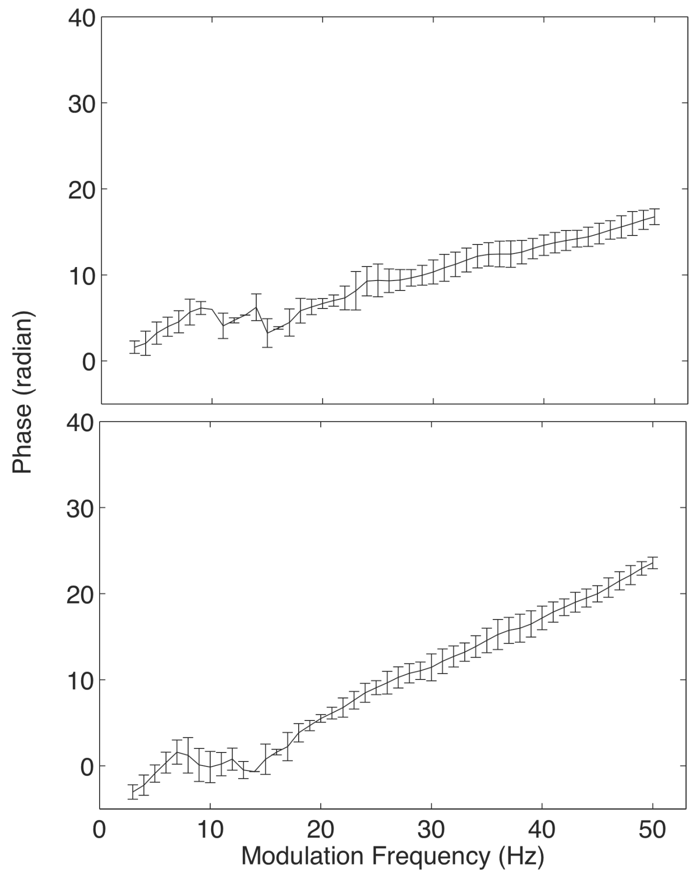

Figure 12: The phase (averaged over different carriers) for each dynamic stimulus with pure-tone carriers (and the relative subject contribution to each). The top panel is the phase from the up sweep stimuli and the bottom panel is the result from down sweep stimuli. The error bars represent the 95% confidence intervals

In Figure 12, the upper panel corresponds to up sweep stimuli and lower panel corresponds to down sweep stimuli. Experimental results show that the results of up sweep stimuli and down sweep stimuli are very distinct. Thus, they are different from each other and no further averaging techniques is used here. The phases in both graphs are linear from 4 – 8 Hz and 20 – 50 Hz. The slopes of both graphs are both gradually decreasing over the whole region, but a more rapid change of slope appears at 25 Hz for up sweep stimuli and 28 Hz for down sweep stimuli. These slopes will be later used to estimate the group delays.

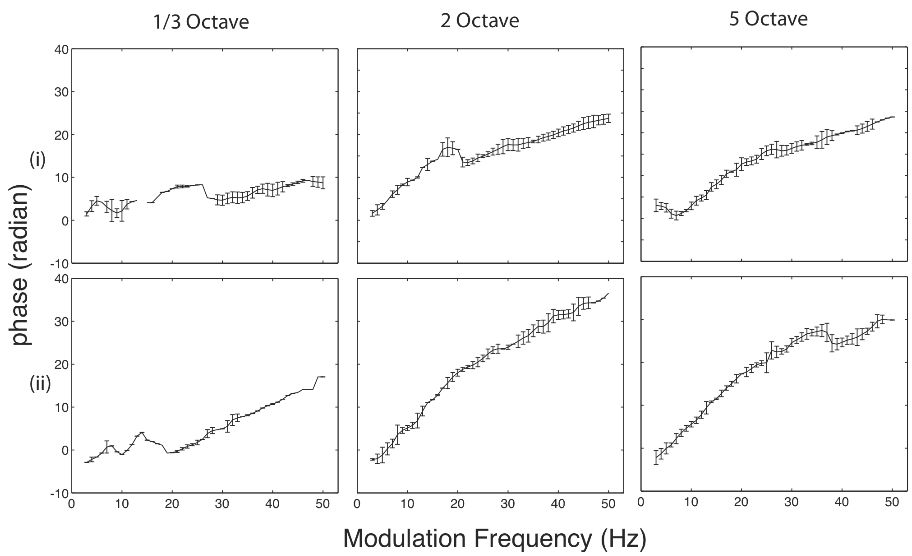

Figure 13: The phase (averaged over subjects) for each dynamic stimulus with pink-noise carriers. The top row (i) is the phase from the up sweep stimuli and the bottom row (ii) is the result from down sweep stimuli. Note that fewer gaps are found in all the results compared to Figure 12 because discontinuous points are estimated using their adjacent data (±1 Hz). The error bars represent the 95% confidence intervals.

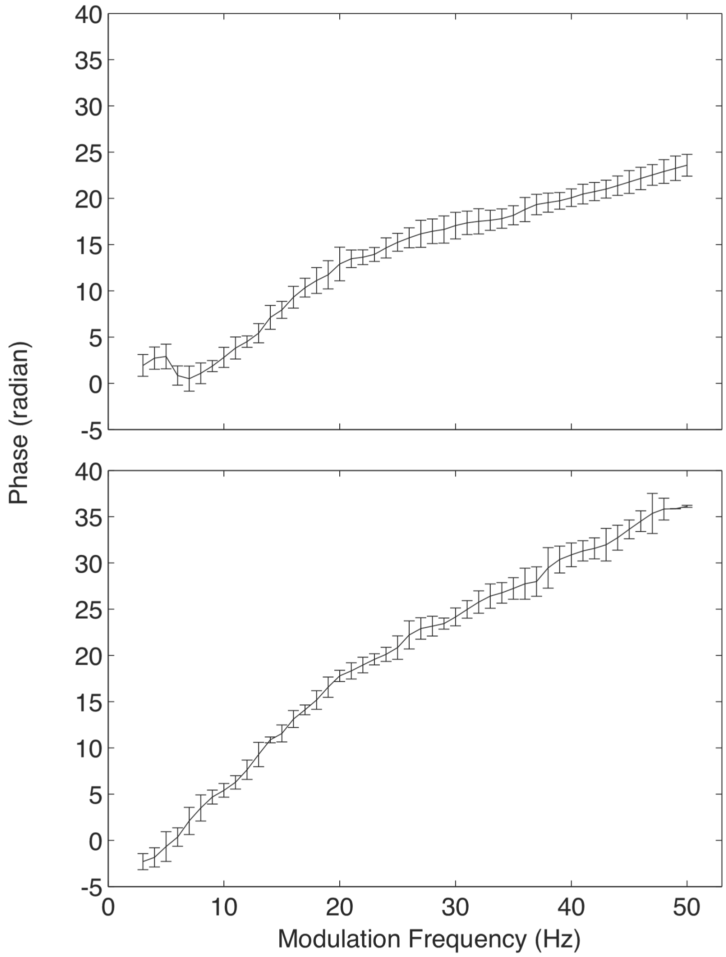

Figure 14: The phase (averaged over different carriers) for each dynamic stimulus with pink-noise carriers (and the relative subject contribution to each). The top panel is the phase from the up sweep stimuli and the bottom panel is the result from down sweep stimuli. The error bars represent the 95% confidence intervals.

Figures 13 and 14 shows the results using pink-noise carriers. They are also approximately linear for many frequencies. The results for pure-tone carriers have a similar shape compared to the result from Alaerts et al in 2009. Both slopes of the graph are gradually decreasing. A change of slope can be seen near 20 Hz.

The group delay and their corresponding error are listed in the following charts. The change of slope at 20 Hz reflects a change of group delay at 20 Hz. This effect appears for all types of stimuli. As we can see, the group delays in 8 – 20 Hz (Row 1) are all over 150 ms, while the group delay in 20 – 50 Hz (Row 2 -4) are around 50 – 100 ms. The large errors in pure tones carriers 8 – 20 Hz are mainly due to the region in 8 – 12 Hz. Note that all the down sweep stimuli (Column 3 and 4) have a larger group delay compared to those using up sweep stimuli (Column 1 and 2). These differences are statistically significant particularly in 20 – 50 Hz.

	Pure-tone up sweep	Bandlimited up sweep	Pure-tone down sweep	Bandlimited down sweep
8 - 20 Hz	175±68 ms	151±18 ms	207±116 ms	186±20 ms
20 - 30 Hz	59±26 ms	70±18 ms	97±14 ms	106±23 ms
30 - 40 Hz	49±15 ms	49±13 ms	90±10 ms	105±23 ms
40 - 50 Hz	52±6 ms	55±3 ms	100±9 ms	83±24 ms

Table 2: Group delay of different conditions in different range of frequency. Column 1 and 2 show the result of up sweep stimuli. Column 3 and 4 show the group delay of down sweep stimuli. Note that the group delays of down sweep stimuli are larger than the group delay of up sweep stimuli.

3.4 Impulse response of group 1 and group 2

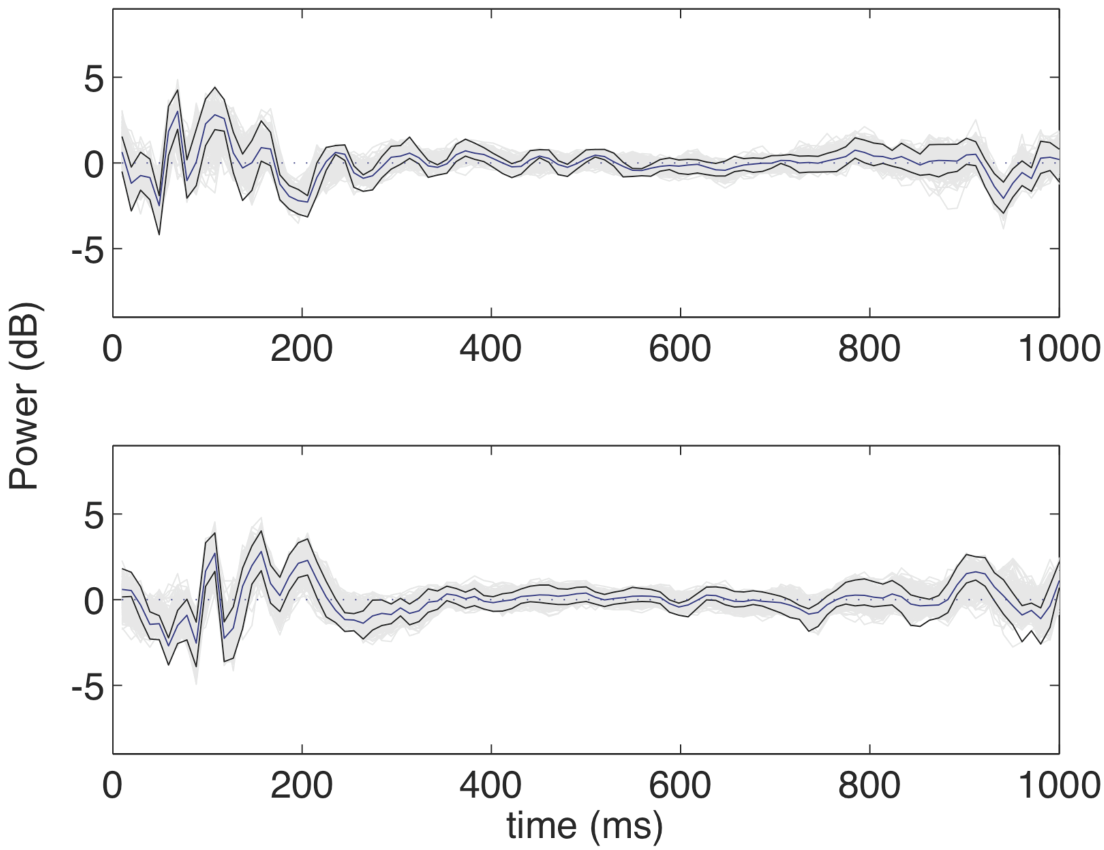

Figure 15: Impulse response calculated using the result from pure-tone carriers. The upper panel is the impulse response calculated from the up sweep stimuli and the lower panel is the impulse response calculated from the down sweep stimuli. The blue is the mean of the impulse response. The grey lines are the individual results from bootstrap (1000 iterations). The black lines show the 95 % confidence interval of the impulse response using BC_a. Several significant peaks are found at 68 ms, 78ms, 156 ms and 196 ms for up sweep stimuli and 78 ms, 127 ms, 196 and 245 ms for down sweep stimuli.

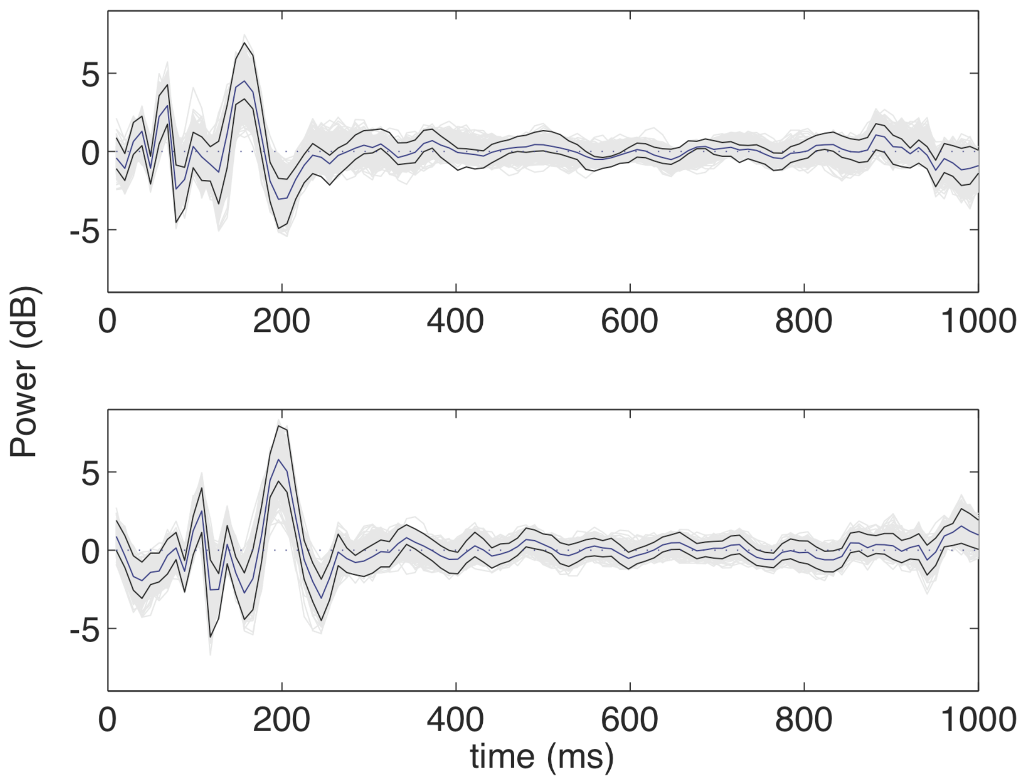

Figure 16: Impulse response calculated using the result from pink-noise carriers. The upper panel is the impulse response calculated from the up sweep stimuli and the lower panel is the impulse response calculated from the down sweep stimuli. The blue is the mean of the impulse response. The grey lines are the individual results from bootstrap (1000 iteration). The black lines show the 95 % confidence interval of the impulse response using BC_a. Several significant peaks are found at 49 ms, 68 ms, 78 ms, 147 ms and 205 ms for up sweep stimuli and 88ms, 107 ms, 127 ms, 196 ms and 245 for down sweep stimuli.

The impulse response of Group 1 and Group 2 are shown in Figures 15 and 16. Since the phases of different sweep have a 180 difference, the impulse responses were separated as up sweep and down sweep. The blue line shows the average of impulse response. The grey region in the background is the result of using bootstrap after 1000 iterations. The confidence interval (solid black lines) after BC_a adjustment explains 90% of the data. In general, there is a strong response at around 100 - 200 ms with frequency around 20-30 Hz. Most of the activities appear in the first 300 ms after the response. In both group 1 and 2, the impulse response of down sweep stimuli is a delayed version of the result of up sweep stimuli. For pure-tone carriers, significant peaks in the first 300 ms for up sweep appear at 68 ms, 78ms, 156 ms and 196 ms. Similar peaks for down sweep appears at 78 ms, 127 ms, 196 and 245 ms. For pink-noise carrier, similar observations are made. The peaks for up sweep stimuli are at 49 ms, 68 ms, 78 ms, 147 ms and 205 ms. While the corresponding peak for down sweep stimuli are at 88ms, 107 ms, 127 ms, 196 ms and 245 ms. In both cases, all peaks are delayed by a minimum of 10 ms. Most of them are delayed by 40 ms. Note that some of the peaks from the impulse response (68 and 78 ms for both up sweeps stimuli. 127, 196 and 245 ms for both down sweeps stimuli) appears at the same time.

Chapter 4: Discussion

This study explores the properties at the low frequency (3 – 40 Hz) MTF using stimuli with different sweep directions and carriers. The data recorded from MEG is analyzed and the MTF from 3 - 50 Hz are calculated. A strong response in the low frequency regions (3 - 10 Hz) is observed. Thus, the shape of the MTF resembles a slightly low pass filter. Besides amplitude, the phases of the response are also calculated. They are approximately linear except the region of 10-20 Hz. The group delay in 30 – 50 Hz for the up sweep stimuli is approximately 55 ms and the group delay of the down sweep stimuli is close to 100 ms. All the group delays calculated in the down sweep stimuli is larger than those in the up sweep cases. Besides the effect of sweep, the group delay increases dramatically in the lower frequency regions (8 - 20 Hz). Impulse responses are calculated using the result of the amplitude and phase. The shape of the impulse response for the down sweep stimuli is delayed compared to the up sweep stimuli. Most of the activity appears around 50-200 ms.

4.1 MTF in the lower frequency region (3-20Hz)

The response of MTF in the low frequency region is prominent when the carrier is wideband pink noise. This prominent response can be found around 3 -12 Hz. It agrees with the previous studies done by Alaerts et al (2009) using EEG, which they found a strong response around 10 Hz and 20 Hz using stationary speech-weighted noise. Other studies also found similar responses (Maiste et al 1989, Picton T.W. 2002). These peaks have been explained by the generation of the

40-Hz peak and the aSSR itself. Galambos et al in 1981 suggested that the 40 Hz peak represents the coalescence of the middle latency responses (MLB). It also explains the shape of the aSSR. Many other studies support this idea (Makeig 1990, Plourde et al 1991, Suzuki et al 1994). While this maybe the generator of ASSR, computer stimulation shows the prediction may not very good (Azzena et al, 1995; Santerelli et al, 1995). The generation of 10-Hz response may also due to the superposition of multiple sources around auditory cortex. This can be related to the studies done by Liégeois-Chauvel et al in 2004 showing different MTF at different locations of auditory cortex based on epileptic patients. Several regions are found to show strong response below 10 Hz and give a shape of a low pass filter. Although they may not necessarily in phase, this provides a possible explanation to our observation. Besides the origin of the 40-Hz peak in the MTF, alpha band activities may also contribute to the strong response at 10 Hz. It is known that a strong 10 Hz response can be recorded if the subject is awake but with eyes closed (Niedermeyer 1999, Robin et al 2002). Thus, this signal may also contribute to the strong response of our MTF.

4.2 The effect of carrier

In our experiment, the pure-tone carriers and pink-noise carriers are used for the stimulus. In the case of the pink-noise carrier, a wider band carrier gives more significant responses at the low frequencies. This can be seen in the bar chart in Figure 8. The ratio of significant responses increase from 0.1 to 0.5 when the frequency band increases from 1/3 to 5 octaves. However, when we compared the significant response of pure-tone carrier and 1/3 octave carrier, they show a different result. In Figures 5 and 8, both pure-tone carriers and the 1/3 octave carrier have less significant response from 10-20 Hz compared to 30-50 Hz; however, the pure-tone carriers still have more significant response compared to 1/3 octave in that frequency range. In the other hand, the subjects in the 5 octave case still outperformed all those in the pure-tone cases. The distribution of the ratio in the pure-tone carrier is actually more comparable to the case with those in the 2 octave carrier, where both of them have a similar distribution of significant responses. Similar comparisons for broadband and narrow band carriers have been done in eliciting AEP-like response (Power et al 2007). They found that a narrow band 2 kHz tone is not as efficient in eliciting AEP-like response compared to modulated broadband noise. Another study (Purcell et al 2004) using a white noise carrier to measure aSSR also found that the white noise carrier generates stronger response in the range of 35 – 60 Hz compared to narrow band carriers. All of their results were similar to what was observed here. One of the classical explanations is the tonotopic nature of the auditory cortex. A narrow band carrier activates a smaller area of the cochlea, and presumably the auditory cortex. Since fewer neurons are driven by the source, the response is weaker and harder to detect. However, this explanation cannot explain the weak responses in the case of the 1/3 octave carrier. If this explanation holds, 1/3 octaves should give a more prominent response compared to a pure-tone carrier. But here are seen the opposite results. One possible explanation is that different carrier bands activate different parts of auditory cortex. Since they are not necessarily in phase, different carrier bandwidths may have different effects whether to cancel or superimpose the signal, and thus give a different number of significant responses. Another possible explanation is that bandlimited noise stimulates a more substantial area of auditory cortex than a modulated tone and at the same time stimulating more specific neural pathways than broadband noise (Power et al 2007).

4.3 The effect of exponential sweep

Exponential sweeps are also used in our experiments and the results are compared to the constant value amplitude modulations. For the first time we exploit the nature of an exponential sweep to measure low frequency MTF. The results are satisfactory for both narrow band and wide band carrier. In all cases, sweeps and constant AM rate stimuli show no significant difference between two conditions, which is similar to all previous studies using linear sweeps (Picton et al 2002, Artieda et al 2003). However, the band around 30 – 50 Hz appears to be flat compared to other studies, which normally give a strong peak at 40 Hz (Roβ et al 2000, Picton et al 2002, Purcell et al 2004). This flat MTF is actually comparable with the study of Alaerts et al (2009). Although their MTF has a slightly low pass shape, the noise of their studies also exhibits the same shape. If noise is subtracted from their results, a flat MTF is most likely to be the cast at 5 – 30 Hz. For the 40 Hz peak, a possible explanation of the difference is the use of sweep conditions. It is plausible that different sweep conditions activate different parts of the auditory cortex in a different order. If different parts of the auditory cortex have a different MTF, then the order of activations will change the MTF. Another point that worth mentioning is that the 37 Hz aSSR measured using sweep stimulus is comparable with the constant stimulus. Thus, the MTFs calculated by sweeps are most likely underestimating the real MTF if there is a peak present at 40 Hz. Although previous research found that stimuli presented using linear sweeps will not affect the result of MTF (Picton et al 2002, Artieda et al 2003), the effect of exponential sweep is not known. In our case, the 40 Hz peak is certainly suppressed. This observation may have potential effects on other research because the 40 Hz region has been used as an indicator of auditory response. If the use of varying AM sweep suppresses the peak at 40 Hz, another indicator has to be used to reduce the effect of varying sweep.

4.4 The shape of the MTF

In Figure 7, where the stimuli are pure-tone carriers, strong response can be found at 3 Hz, 10 Hz and 20 Hz. 10 Hz and 20 Hz strong response have been reported under different situations, but the strong response at 3 Hz is not reported from previous studies. When the stimuli are changed to broadband pink noise, the peak at 10 Hz become more prominent. In the case of wide band carrier, the MTF exhibits a slight low pass shape at around 10 Hz. The strong response at around 3-10 Hz appears in both the pure-tone carrier and broadband carrier. This strong response at low frequency regions can possibly explained by the sensitivity of low frequency envelope. Since human speech is mostly modulated around 1-10 Hz, a strong response at the low frequency region may presumably facilities the need of speeches perceptions.

4.5 <u>The group delay of the response</u>

The group delay of the up sweep carrier is close to 50 ms at 20-50 Hz (Table 2). This result agrees with MEG studies about group delay. The group delay found by Roberts (2000) is 72 ms at 20 Hz and 48 ms at 40 Hz. Another recent study using EEG also showed the group delay at 28-32 Hz to be 31 ± 9 ms. However, for the down sweep carrier, the group delay increases to 90 ms. This effect of sweep directions has never been reported. The only related result found was the latency of the response decreases consistently with increasing carrier frequency (Picton T.W. et al 2003). However, the relationship between sweep directions and group delay was not explored before. Actually, except the data from narrow band carriers for 8-20 Hz, all down sweep data have a statistically larger group delay compared to the group delay of up sweep data. Our finding shows that, if presumably both stimuli stimulate the same part of the auditory cortex, down sweep stimulus is processed slower than the up sweep stimuli. While the reasons of this observation remain unknown, it is possible that there are multiple origins of the signals contribute to our results. If each origin corresponds to a system that process the signals in the auditory cortex, then there may be different group delay for each of the systems. And thus the group delay of the auditory cortex will depend on the history of the signal. This hypothesis is consistent with the result of our flat MTFs in the region of 20 – 50 Hz. While previous studies explained the average response of the auditory system, our studies may explore some specific parts of the auditory system that depends on the order of stimuli frequencies. If different parts of the auditory cortex have a different group delay and modulation characteristics, it is likely that our stimuli trigger those parts in a different order and thus give a different group delay and MTFs.

For frequencies below 20 Hz, the group delay increase to 100 ms. The group delay in this region has been reported by different studies before. Rees et al in 1986 found that the group delay in 1 – 4 Hz is in the range of 80 – 180 ms. Maiste and Picton in 1989 found the apparent latency from 3.9 – 6.5 Hz to be 125 ms using FM stimuli. Our results show that the group delay from 8 – 20 Hz is 151±18 ms for up sweep stimuli and 186±20 ms for down sweep stimuli. These estimations match the result of previous studies. While the reasons of the increase group delay remain unknown, it is widely believed that the group delay increases below 20 Hz. Our results from the slope of the phases also support this argument.

In Figures 11 and 13, the slopes of the phase change in different frequencies. In all the cases, slope decreases gradually, implying the group delay decreases with increasing frequency. Although the generally trend of the slope is decreasing, the slope of some regions vary. These “ripples” of phase appear almost every 3-6 frequency bins from 15 Hz to 30 Hz. Some particular strong “ripples” include 10 – 14 Hz, 18 – 22 Hz, 28 - 32 Hz, 34 – 38 Hz and 48 – 52 Hz. In all these regions, group delay decrease dramatically then climb up again as the frequency increases. Alaerts et al (2009) found the same in one of the regions, namely 28 - 32 Hz. From their graph, there are also ripple appear at 18 - 22 Hz. However, the changes at other frequency regions were not found in their results. This subtle rippling effect makes the estimation of group delay at particular frequency difficult because the estimation is very sensitive to the slope of the phase. One of the simple explanations is that they might be completely random or induced by population. Since we are only measuring the group delay from small samples, unless the sample size is sufficiently large, the mean of the phase will not exactly become a straight line. However, the results from Alaerts et al and us share some similar regions. And some of these “ripples” are strong enough to be considered as a change of group delay. Thus, it is possible that group delay changes more frequently then what we thought.

Between 7 -15 Hz, the phase is particularly noisy due to the weak aSSR measured in this frequency band. Since our denoising algorithm based on the amplitude (power) of the response, the low significant responses in this frequency band directly affect the data acquisition in this area. Thus, large errors are found in these frequency regions. This issue can be possibly fixed by using phase coherence as the criteria of denoising. Similar work has been done by Picton (2001) and showed promising results with phase coherence. However, this possible improvement may be hindered by the use of exponential sweep. Since our stimuli are exponentially varying, the phases of the stimuli also changes. Thus, the phases of the subjects response also changed. Mathematically, this problem can be solved by taking the difference between the phase of the response and that of the input stimulus; however, this gives extra uncertainty to the data since little is known about the cortical response of varying phase. And this uncertainty may also be carried to the phase coherence of the subjects.

4.6 The Impulse response from the instantaneous aSSR

The impulse response of the auditory system to a modulated stimulus has been found before by Power et al (2007) using Auditory Evoked Spread Spectrum Analysis (AESPA), which was originally used in finding the impulse response of vision (Lalor et al 2006). Others normally examine Auditory Evoked Potentials (AEP), which can be generated by repeated presentation of click/tone. Our impulse responses for up sweep and down sweep stimuli are similar, but the shape of down sweep is a delayed version of the up sweep. This probably reflects the increase of group delay in different frequency regions using down sweep. From the impulse response, most neural activities appear in the first 200 ms. Several prominent peaks are also found. The method used here showed a potential method to generate impulse responses. Since amplitude and phase are both available under favorable conditions, one can generate a more precise impulse response of the auditory system. This can be done by acquiring better data set for low frequency, especially in the range of 7 - 15Hz, which gives a small number of significant subjects in our experiment.

Chapter 5: Conclusion

The low frequency MTF is measured using exponentially varying modulated stimuli. The results show a prominent response in the lower frequency band at around 3 Hz to 20 Hz. Thus the MTFs have a slight low pass shape. High variability within subjects is found in the range of 10 – 20 Hz because of small number of significant subjects. The directions of sweep also play an important role here. The group delay of the response increases from 50 ms to 100 ms when the stimuli changed from up sweep to down sweeps. The effects of different carriers were also showed here. While 5 octave pink noise gives the most significant number of subjects for different frequencies from 6 - 30 Hz, pure-tone carrier stimuli have approximately the same number of significant subjects as the 2 octaves stimuli. In the other hands, subjects respond weakly to the stimuli with 1/3 octave. Other frequency ranges are not strongly affected by the carrier bandwidth.

Group delay of the cortical response varies with different stimuli. In the low frequency regions, the responses from down sweep stimuli have a longer group delay compared to those from the up sweep stimuli. The impulse response was also calculated from the amplitude and phase information. Most of the activities appear for the first 200 ms after the stimulus. The impulse response of down sweep stimuli is also delayed compared to the result from up sweep stimuli.

Bibliography

Alaerts J. Luts H., Hofmann, M., Wouters J. Cortical audiotry stead-state responses to low modulation rates. International Journal of Audiology 2009. 48: 582-593.

Aoyagi M, Fuse T, Suzuki T, Kim Y, Kokie T. An application of phase spectral analysis to amplitude-modulation flowing response. Acta Otolaryngol (Stockh) 1993a; 504(Suppl):82-88.

Aoyagi M, Kiren T, Kim Y, Suzuki Y, Fuse T, Kokie Y. Optimal modulation frequeny for amplitude-modulation following response in young children during sleep. Hear Res 1993b;65;253-261.

Aoyagi M, Kiren T, Kim T, Suzuki Y, Fuse T, Koike T. Frequency specificity of amplitude-moduation following response deteted by phase spectral analysis. Audiology 1993c;32:293-301.

Artieda J, Valencia M, Alegre M., Olaziregi O., Urrestarazu E., Iriarte J. Potentials evoked by chirp-modulated tones: a new technique to evaluate oscillatory activity in the auditory pathway. 2004. Clinical Neurophysiology. Vol. 115 Issue 3. pp 667-709.

Azzena GB Conti, Santerelli R, Ottaviani, Paludetti G, Maurizi M. Generation of human auditory steady-state responses. I: Stimulus rate effecs. Hear Res 1995;83:1-8.

Bohorquez J, Ozdamar O. Generation of the 40-Hz auditory steady-state response (ASSR) explained using convolution. Clinical Neurophysiology 119. 2008. Elsevier. 2598-2607.

Ding N. and Simon J.Z. Neural representations of complex temporal modulations in the human auditory cortex, J Neurophysiol 102. 2009. 2731-2743

Efron B, Tibshirani, R.J. An Introduction to the Bootstrap. Chapman & Hall/CRC. 1998. 184-188.

Farina A, Simultaneous measurement of impulse response and distortion with a swept-sine technique. Preprint of the AES 108th Convention, Paris, February 2000.

Fisher N.I. Statistical analysis of circular data. Cambridge University Press. 2000. pp 31 -33.

Galambos R, Makeig S, Talmachoff PJ. A 40-Hz auditory potential recorded from steady-state the human scalp. Proc Natl Acd Sci USA 1981; 78:2643-7

Hamalainen M., Hari, R. Ilmoniemi R.J., Knuutila J. and Lounasmaa O.V. Magnetoencephalography – theory, instruemetation, and applications to noninvasive studies of the working human brain. Review of modern Physics, Vol. 65. No. 2. April 1993. 413-497.

Hari R., Levanen S., Raij T. Timing of human cortical functions during cognition: role of MEG. Trends in Cognitive Sciences. Elsevier Sicnece Ltd. 2000 Dec 1;4(12):455-462.

Lalor E.C., Pearlmutter B. A., Reilly R. B., McDarby G., Foxe J. J. The VESPA: A method of rapid estimation of a visual evoked potential. NeuroImage 32 2006. 1549-1561.

Liégeois-Chauvel C., Lorenzi C., Trébuchon A, Régis J., Chauvel P. Temporal Envelope Processing in the Human Left and Right Audiotry Cortices. Cerebral Cortex. July 2004;14:731-740.

Lins O.G., Picton T.W. Auditory steady-state responses to multiple simultaneous stimuli. Electroencephalography and clinical Neurophysiology 96. 1995. 420-432.

Luo, H., Y. Wang, D. Poeppel and J. Z. Simon. Concurrent Encoding of Frequency and Amplitude Modulation in Human Auditory Cortex: An Encoding Transition, J Neurophysiology, 98. 2007. 3473-3485.

Makeig S. A dramatic increase in the auditory middle latency response at very slow rate. In Brunia C, Gaillard A, Kok A, editors. Psychophysiological brain research; 1990 p. 56-60

Niedermeyer E. The normal EEG of the waking adult. In: Niedermeyer E and Lopes da Silva F (eds). Electroencephalography: Basic Principles, Clinical Applications, and Related Fields. Baltimore: Williams and Wilkins; 1999, pp. 149–173.

Picton T.W., Dimitrijevic A., John M. S., Roon P. V. The use of phase in the detection of auditory steady-state responses. Clinical Neurophysiology. 2001. 112:1698-1711.

Picton T.W., Sasha Joh M., Dimitrijevic A., Purcell D. Human auditory steady-state responses. International Journal of Audiology. 2003. 42:177-219.

Plourde G, Stapells DR, Picton TW. The human auditory steady-state evoked potentials Acta Otolaryngol Suppl (Stockh) 1991;491:153-160

Poeppel D. The analysis of speech in different temporal integration windows: cerebral lateralization as 'asymmetric sampling in time'. Speech Commun 41: 245–255, 2003.

Poulsen C., Picton T.W., Paus T. Age-Related Changes in Transient and Oscillatory Brain Responses to Auditory Stimulation in Healthy Adults 19-45 Years Old. 2007. Cerebral Cortex. June 2007. 17:1454-1467.

Purcell D.W., John S.M., Schneider B.A., Picton T.W. Human temporal audiotry acuity as assessed by envelope following responses. J Acoust Soc A. 2004.116: 3581-2593.

Power A.J., Lalor E.C., Reilly R.B. Eliciting Audio Evoked Potentials Using Continuous Stimuli. Proceedings of the 29th Annual International Conference of the IEEE EMBS. 2007. 4264–67.Roβ, B., Borgmann, C., Draganova R., Roberts L.E., Pantev, P. A high-precision magnetoencephalographic study of human auditory steady-state responses to amplitude-modulated tones. J. Acoust. Soc. AM 108(2). August 2000.679-91. NeuroReport. December 20 2002; Vol.13 No 18. 2487-2492.

Regan D. Human brain electrophysiology: evoked potentials and evoked magnetic fields in science and medicine. Amsterdam Elsevier. 1989.

Robin I.G., John M.S., Jerome E. Jr. Mark S.C. Simultaneous EEG and fMRI of the alpha rhythm.

Schoonhoven R, Boden C.J.R., Verbunt J.P.A., Munck de J.C. A whole head MEG study of the amplitude-modulation-following response: phase coherence, group delay and dipole source analysis. Clinical Neurophysiology 114. 2003. Elsevier. 2096-2106.

Suzuki T, Kobayashi K, Umegaki Y. Effect of natural sleep on auditory steady state responses in adult subjects with normal hearing. Audiology 1994;71:460-468

Xiang, J., Y. Wang and J.Z. Simon. MEG Responses to Speech and Stimuli with Speechlike Modulations, Neural Engineering, 2005. Conference Proceedings. 2nd International IEEE EMBS Conference on, 33-36.